CrystEngComm

Accepted Manuscript

ROYAL SOCIETY OF CHEMISTRY

www.rsc.org/crystengcomm

Journal Name

RSCPublishing

ARTICLE

On the nature of M–CO(lone pair)···π(arene) interactions in the solid state of fluorinated oxaphosphirane complexes†‡

Cite this: DOI: 10.1039/x0xx00000x

Received 00th January 2012,
Accepted 00th January 2012

DOI: 10.1039/x0xx00000x

www.rsc.org/

Cristina Murcia-García,[a] Antonio Bauzá,[b] Antonio Frontera,[b,*] and Rainer Streubel[a,*]

We have recently communicated [*CrystEngCommun* 2015, **17**, 1769–1772] the synthesis and X-ray characterization of several oxaphosphirane tungsten(0) complexes especially designed to analyse the intramolecular W–CO(lone pair)···π(arene) interaction varying the degree of fluorination in the arene. Unexpectedly, the phenyl substituted oxaphosphirane complex showed the shortest CO···π distance in the solid state and very close to the one observed for the pentafluorophenyl derivative. Other complexes with two or three fluorine substituents exhibited longer distances. We rationalized the affinity of the M–CO moiety for both electron rich and electron deficient rings by considering that the interaction can be also understood as a π–π interaction where the negative part of the CO is dominant in the π-acidic arene and the positive part of the CO is dominant in the π-basic arene. This explanation was supported by DFT calculations using orbital analysis and the Bader's theory of "atoms-in-molecules". Herein we expand the previous study with new theoretical results of some model complexes to gain insight into the energetic and geometric features of the interaction. The experimental behaviour of the ^{31}P-NMR chemical shifts of the title compounds agrees well with previous theoretical explanation of the physical nature of the interaction. Furthermore, we analyse the crystal packing of the four X-ray structures previously communicated in order to scrutinize other interactions in the solid state that may influence the W–CO···π interaction. Finally, stronger intermolecular interactions that influence the crystal packing are also analysed using DFT calculations.

1. Introduction

The instrumentation of many chemical and biological processes is often dominated by an intricate combination of non-covalent interactions.[1] Therefore the correct description of the interactions between molecules is needed for the continuous progress of the supramolecular chemistry[2] that usually relies on strong and directional interactions such as hydrogen and halogen bonding, and less directional forces like ion pairing. Moreover, non-covalent interactions involving aromatic rings are enormously significant in this field.[3] They play important roles in chemistry and biology, in particular drug–receptor interactions, crystal engineering, enzyme inhibition and protein folding.[4] For instance, lone pair–π interaction, which takes place between lone-pair bearing electronegative atoms of the neutral molecules and π-acidic aromatic systems, is a counterintuitive intermolecular force in supramolecular chemistry.[5] In particular, the Ch–π (Ch = O, S, Se and Te) interaction has been discussed in detail.[6] In some relevant examples the oxygen atom provides the lone pair including water,[7] ether,[8] or carbonyl moieties.[9] Theoretical calculations of the energetic features of interactions between oxygen (lone pair) and aromatic rings demonstrate that the interaction is enhanced in the presence of π-acidic rings like hexafluorobenzene.[10] However, even electron-rich aromatic rings and oxygen lone pairs also exhibit weak attractive interactions.[11] More recently, it has been demonstrated that M–CO(lone pair)···π(arene) interactions are relevant in the X-ray structures of a number of transition organometal carbonyl derivatives.[12] M–CO(lone pair)···π(arene) interactions lead to well-defined supramolecular architectures. Such interactions are needed to have a complete understanding of the way this type of organometallic molecules associate in the solid state.[12] As a matter of fact, a search of the Cambridge Structural Database (CSD)[13] using the criteria shown in Scheme 1 has demonstrated the presence of several supramolecular motifs. These have been divided in (i) zero-dimensional (two molecules aggregate) motifs, (ii) one-dimensional aggregation patterns (e.g. linear, zigzag or helical supramolecular chains), and (iii) three-dimensional architecture. In total, the number of

structures (considering any transition metal) exhibiting this interaction was limited to 85.[12b]

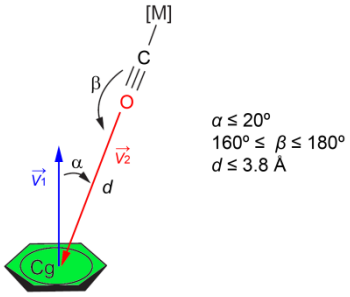

Scheme1 Diagram illustrating the search protocol used by Zukerman-Schpector *et al.*[12b]

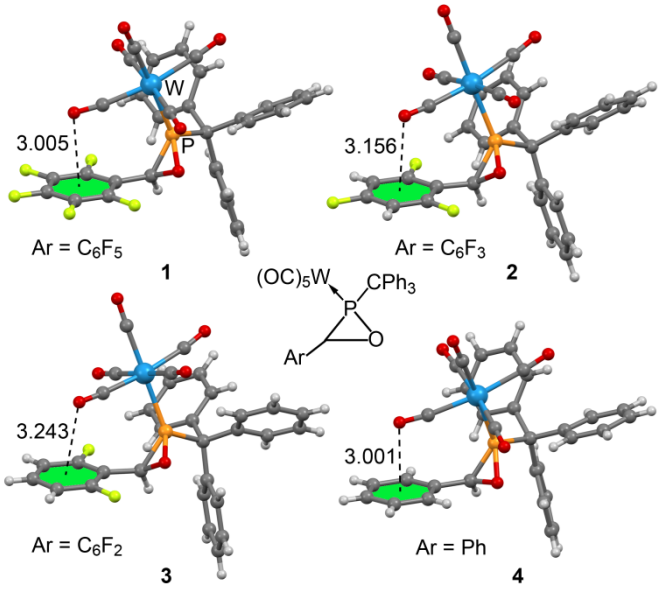

Fig. 1 X-ray structures of compounds **1**–**4**.

Taking advantage of the experience of some of us in the chemistry of oxaphosphirane rings,[14] we have recently communicated[15] the design synthesis and X-ray characterization a series of complexes exhibiting close M–CO···π intramolecular contacts (see Fig. 1) where we tuned the electronic nature (π-acidity/basicity) of the π-system by using aromatic rings with different degree of fluorination. As a result we found that the M–CO···π intramolecular distance increases as the degree of fluorination decreases, apart from phenyl ring that unexpectedly exhibited the shortest distance. We rationalized the affinity of the M–CO moiety for both electron rich and electron deficient rings by considering that the interaction can be understood as a π–π interaction where the negative part of the CO is dominant in **1** (π-acidic arene) and the positive part of the CO is dominant in **4** (π-basic arene). In this manuscript we provide additional theoretical results to further rationalize this point. We report new high level DFT calculations in order to gain knowledge into the geometric and energetic features of the CO···π complexes of three different aromatic rings with free and metal-coordinated carbonyl and considering several binding modes. Moreover, we have also examined the CSD expanding the search in order to include those X-ray structures where the interaction with the CO moiety resembles a π–π interaction. The previously reported CSD search commented above restricted the β angle between 160º and 180º values. Therefore those structures with M–CO···π interactions resembling **1**–**4** were not considered (small β angles).

2.6. Theoretical methods

The geometries of the complexes included in this study were computed at the BP86-D3/def2-TZVP level of theory using the crystallographic coordinates within the TURBOMOLE program.[16] This level of theory that includes the latest available dispersion correction (D3) is adequate for studying non-covalent interactions dominated by dispersion effects like π-stacking.[17] The basis set superposition error for the calculation of interaction energies has been corrected using the counterpoise method.[18] The "atoms-in-molecules" (AIM)[19] analysis of the electron density has been performed at the same level of theory using the AIMAll program.[20]

3. Results and discussion

3.1. Preliminary study

We have optimized the complexes shown in Fig. 2 in order to study the influence of the electronic nature of the ring (benzene, hexafluorobenzene and 1,3,5-trifluorobenzene) on the strength of the interaction. In addition, we have studied three different binding orientations for the free CO (complexes **5**–**13**) and two binding modes for the W-complexed CO (complexes **14**–**19**).

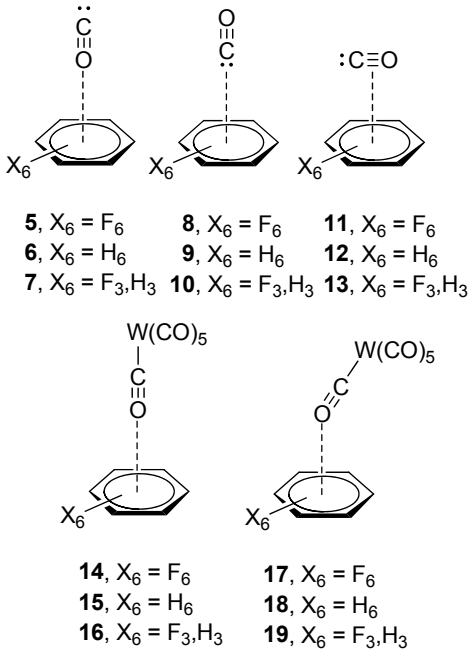

Fig. 2 Complexes **5**–**19** studied in this work

Table 1. Interaction energies with BSSE correction (ΔE, kcal/mol) and equilibrium distances[a] (R_e, Å) for **5-19**.

Complex	Symm.	ΔE	R_e
5 ($C_6F_6\cdots O{\equiv}C$)	C_{6v}	–1.6	3.080
6 ($C_6H_6\cdots O{\equiv}C$)	C_{6v}	–0.6	3.154
7 ($C_6H_3F_3\cdots O{\equiv}C$)	C_{3v}	–1.2	3.123
8 ($C_6F_6\cdots C{\equiv}O$)	C_{6v}	–1.2	3.243
9 ($C_6H_6\cdots C{\equiv}O$)	C_{6v}	–0.6	3.278
10 ($C_6H_3F_3\cdots C{\equiv}O$)	C_{3v}	–0.9	3.269
11 [$C_6F_6\cdots$(CO)]	C_s	–1.7	3.249
12 [$C_6H_6\cdots$(CO)]	C_s	–1.9	3.268
13 [$C_6H_3F_3\cdots$(CO)]	C_s	–1.7	3.274
14 ($C_6F_6\cdots O{\equiv}CW$)	C_2	–1.8	3.008
15 ($C_6H_6\cdots O{\equiv}CW$)	C_2	–0.9	3.132
16 ($C_6H_3F_3\cdots O{\equiv}CW$)	C_s	–1.3	3.062
17 ($C_6F_6\cdots O{\equiv}CW$)	C_s	–2.4	3.036 (3.021[b])
18 ($C_6H_6\cdots O{\equiv}CW$)	C_s	–3.2	3.155 (3.107[b])
19 ($C_6H_3F_3\cdots O{\equiv}CW$)	C_s	–2.0	3.283 (3.078[b])

[a]Distances to the ring centre. [b]Distance to the ring plane

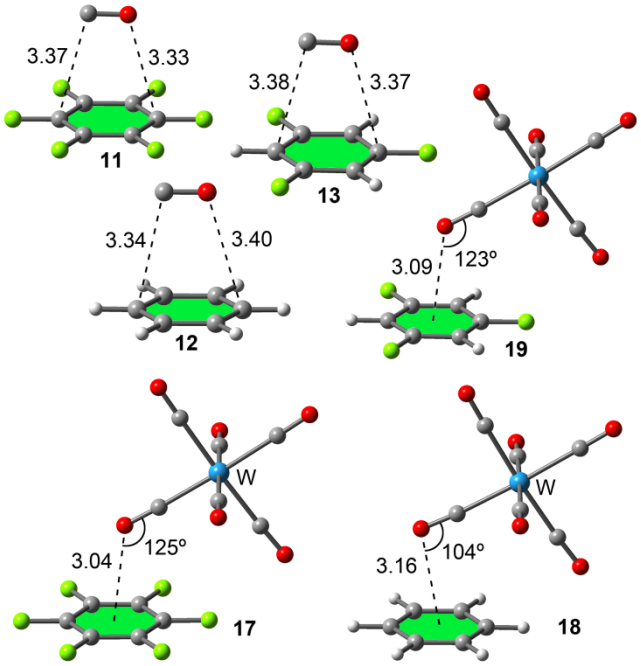

Fig. 3 Optimized complexes **11**–**13** and **17**–**19**. Distances in Å.

The energetic and geometric results are summarized in Table 1 and some interesting issues arise from the inspection of the results. First, the interaction is weak (< 2 kcal/mol) in all complexes apart from **17** and **18**. Second, the examination of the interaction energies in complexes **5**–**10** (CO located along the main symmetry axis) reveals that hexafluorobenzene (π-acidic ring) presents more favourable interaction energies than trifluorobenzene and benzene. Latter ring exhibits the weakest interaction energies. However in complexes where the CO is disposed parallel to the ring plane (**11**–**13**), the benzene complex is the most favourable. The optimized geometries of these complexes are shown in Figure 3 and it can be observed that the CO is almost parallel to the ring plane, resembling a π-stacking interaction. In complex **12** (electron rich ring), the C end of the C≡O is closer to the ring and the O end is closer in complex **13** (electron poor). The AIM study (focused to the analysis of ρ values at the bond critical points, see ESI) agrees well with this explanation. More interestingly, the energetic and geometric results obtained for $W(CO)_6$ complexes **14**–**19** clearly show that the most favoured orientation corresponds to β < 180º (see Fig. 3, complexes **17**–**19**). Moreover the most favourable interaction corresponds to the benzene complex **18** (β = 104º) that adopts a geometry resembling the X-ray structure (see Fig. 1). The geometry of the hexafluorobenzene and trifluorobenzene complexes **17** and **19** also show small β angles (125º and 123º, respectively) indicating a preference for this orientation instead of the perpendicular one.

3.2. Cambridge Structural Database search

As stated above the M–CO(lone pair)···π(arene) interaction in the model complexes shows preference for small β angles. However the CSD analysis previously reported in the literature[12b] restricted the search to large β angles (see scheme 1) and, conversely, it allowed long Cg···OC–M distances (up to 3.8 Å). We have re-analyzed the CSD in order to include low β angles in the search and to investigate if there is a preference for low angles, focusing our attention in intramolecular contacts. We have also performed the same search examining only intramolecular W–CO···π contacts to compare the geometric features of the hits to those reported herein. For the search we have used the following protocol: $90º \le \beta \le 180º$; $d <$ 3.3 Å and only those hits with "no errors" and "no disorder" in their X-ray structures were considered. In Table 2 we show the number of structures (N) obtained for both inter and intra-molecular searches. Taking into consideration that only the W metal has been considered in the search, a significant number of structures exhibiting the lp–π interaction has been found. Moreover, it can be observed (see Table 2) that there is a strong preference for β angles ranging from 100º to 120º in good agreement with the optimized geometries of complexes **17**–**19** (see Fig. 3). Interestingly, the number of structures with $\beta >$ 160º is only 6, in line with the previously reported analysis of the CSD.[12b] However the large number of structures showing intermolecular contacts for $\beta <$ 140º clearly confirms the relevance of this interaction in the structures of transition organometal carbonyl derivatives leading to well-defined supramolecular architectures (*vide infra*).

Table 2. Number of structures (N) depending on the β (º) angle showing W–CO···π short contacts.

β range	*N* (inter.).	*N* (intra.)
90–100	4	70
100–110	27	19
110–120	17	8
120–140	13	2
140–160	9	0
160–180	6	0
total	76	99

For the X-ray structures showing intramolecular W–CO···π contacts, there is also a strong preference for small angles ($\beta <$

110º, see Table 2), due to their intramolecular character. For this search we have represented the histogram plot of the O···Cg distance (d, defined in Scheme 1) in Fig. 4. It can be observed that most of hits are found for *d* values ranging from 3.1 to 3.2 Å. There are few hits where the d values are shorter than 3.05 Å, therefore the X-ray structures of compounds **1** and **4** are quite exceptional in this sense. The CSD codes of both searches are included in the ESI.

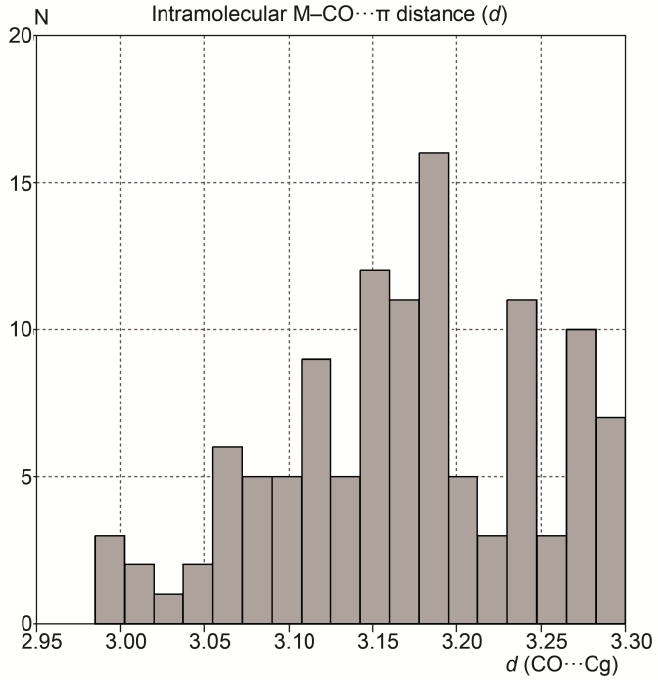

Fig. 4 Histogram plot for *d* parameter (for the definition of *d*, see Scheme **1**)

In Fig. 5 we have selected several hits in order to illustrate the importance W–CO···π interactions in the solid state. In the first example (CSD ref. code DUWNEP),[21] a self-assembled dimer is formed in the solid state where two equivalent W–CO···π interactions are established. In the second one (CACLUN),[22] a 1D infinite chain if formed in the crystal packing where the W–CO group of one molecule establishes a bifurcated CO···π_2 interaction with the adjacent molecule. We have also included in Fig. 5 two selected examples of intramolecular W–CO···π interactions (SOMRAP[23] and BIMHEM[24]). In one of both (SOMRAP), two equivalent interactions are formed where two symmetrically related CO and aryl groups participate.

3.3. ^{31}P–NMR chemical shifts

In our pervious communication, we proposed that W–CO···π contact in complexes **1**–**4** can be defined as π–π stacking interaction to rationalize the fact that both the π–electron poor pentafluorophenyl and π–electron rich phenyl substituted oxaphosphirane complexes (**1** and **4**) present the shortest W–CO···π distances. We also suggested that the negative end of the metal-coordinated CO is dominant in the π-acidic arene (**1**) and the positive part is dominant in the π-basic arene (**4**). This explanation was supported by DFT calculations, including "atoms-in-molecules" and NBO analyses. Moreover, this explanation also agrees with the experimental ^{31}P NMR chemical shifts observed in compounds **1**–**4**, which are summarized in Table 3. We have also included in Table 3 the experimental ^{31}P–NMR chemical shift of a model oxaphosphirane compound for comparison purposes. In this model the arene has been replaced by an alkyl chain (propyl) and, consequently, the W–CO···π contact is not present. Interestingly, it can be observed that compound **1** presents the ^{31}P–NMR chemical shift at higher field than the model, which is a counterintuitive result taking into account the electron withdrawing character of the pentafluorophenyl ring. Strikingly, the contrary is found in compound **4** that exhibits the ^{31}P–NMR chemical shift at lower field than the model complex, indicating that this phenyl ring is behaving as an electron-withdrawing group. A likely explanation is that the W–CO···π interaction is influencing the ^{31}P–NMR chemical shift. That is, in complex **1** the charge transfer from the CO group to the π-acidic C_5F_5 ring causes a concomitant induction effect through the σ-bonds that decreases the ^{31}P NMR

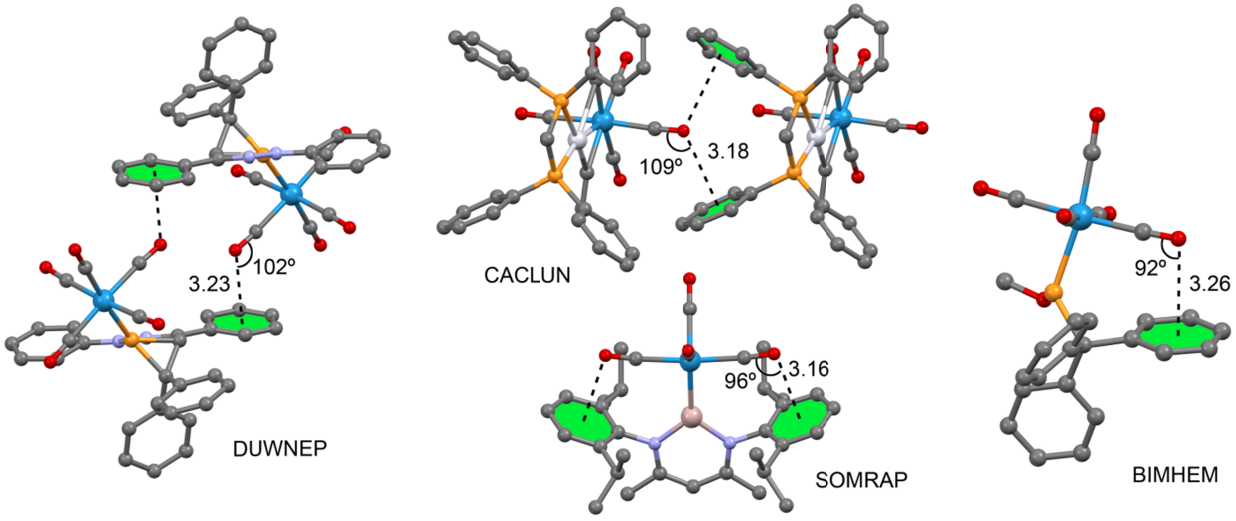

Fig. 5. Partial view of several X-ray structures exhibiting W–CO···π contacts. In capital letters the CSD reference codes are indicated. Distances in Å.

chemical shift. Since in compound **4** the charge transfer is from the π-basic ring to the CO group, the contrary induction effect increases the ^{31}P–NMR chemical shift. In the other rings (compounds **2** and **3**) the differences in ^{31}P–NMR chemical shifts with respect to the model compounds are smaller, in agreement with the weaker W–CO···π interaction.

Table 3. ^{31}P-NMR chemical shifts (ppm) and P–W coupling constants J of compounds **1**–**4** and a model oxaphosphirane having a propyl chain instead of an arene ring (without W–CO···π contacts).

Compound	^{31}P–NMR (ppm)	$^{1}J_{P,W}$ (Hz)
1	7.5	320
2	8.5	316
3	8.9	314
4	16.0	311
Model	10.1	303

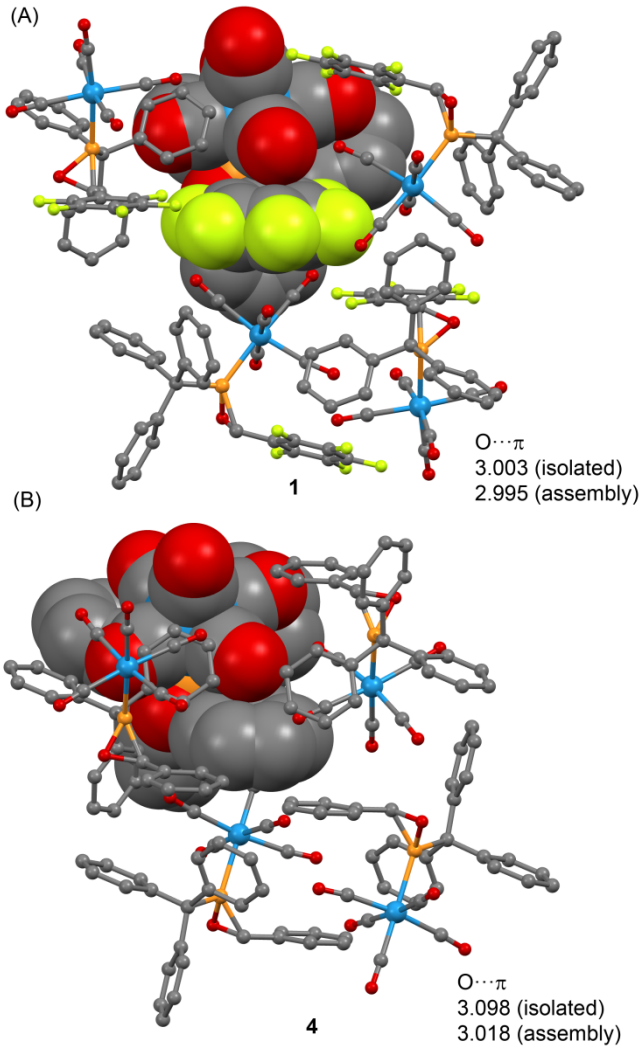

Fig. 6. Partial view of the crystal packing of **1** and **4**. The reference molecule is represented in space filling format. The neighbouring molecules that are located at less or equal then the ΣvdW radii + 0.25 Å are also represented in ball and stick.

3.4. Influence of additional interactions on the W–CO···π

At this point, it should be emphasized that the experimental W–CO···π distances observed in the solid state structures of compounds **1**–**4** (see Fig. 1) can be influenced by other interactions. Therefore we have further analysed the crystal packing of complexes **1** and **4** in order to investigate if the CO and aryl groups participate in other noncovalent interactions which could influence the W–CO···π distance. We have represented in Fig. 6 a partial view of their crystal packing paying attention to the short contacts involving the CO and arene groups (represented in space filling). In this exploration we have considered that short contact between two atoms exists if they are separated by a distance that is less or equal to the sum of the van der Walls radii + 0.25 Å. In both compounds **1** and **4**, four surrounding molecules satisfy this criterion (see Fig. 6). In order to investigate if the W–CO···π distance is influenced by the neighbouring molecules, we have optimized the oxaphosphirane complexes **1** and **4** isolated and in the presence of the four neighbours. Since we have used a high level of theory (BP86-D3/def2-TZVP), the optimization of the whole assembly is computationally unapproachable (e.g. 300 atoms for the assembly of **1**). Therefore, we have used a theoretical model, where some parts of the neighbouring molecules have been simplified (see ESI for details and the structure of the optimized models, Fig. S2). Using this approach, we have optimized the W–CO···π distance and the results are shown in Fig. 6. It can be observed that the optimized distance (measured from the O atom to the ring centroid) using either the isolated molecule or the assembly is very similar (0.008 and 0.070 Å shorter in the assemblies than in the isolated moelcules for **1** and **4**, respectively). These results evidence that the short W–CO···π contacts observed in the solid state of **1** and **4** are not likely due to crystal packing effects.

3.5. Crystal packing and strong intermolecular interactions

We have also evaluated the intermolecular interactions that govern the crystal packing in compounds **1**–**4**. In the case of compound **1** the packing is basically governed by intermolecular W–CO···π and W–CO···H–C interactions. Infinite zig-zag 1D columns (see Fig 7A) are formed in the solid state stabilized by two different W–CO···π interactions, one involving the trityl group and the other one the phenyl substituent of the oxaphosphirane ring. The 1D column is further stabilized by W–CO···H–C hydrogen bonds that involve the H atom of the oxaphosphirane and the coordinated CO (see Fig 7B). These 1D columns interact to each other by means of additional W–CO···π and W–CO···H–C hydrogen bonds generating 2D layers. We have evaluated the interaction energy of a dimer as a representative model, which is large and negative due to the contribution of long range dispersion interactions in addition to the individual contacts marked in Fig. 7B. Interestingly the distance of W–CO···π interaction that implies the phenyl substituent (3.21 Å, see Fig. 7A) is very similar to the theoretical one (see Table 1, complex **16**).

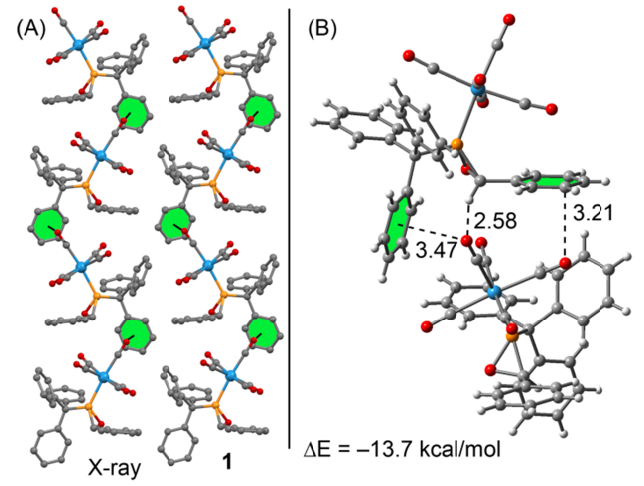

Fig. 7 (A) Partial view of the crystal packing in **1**. H-atoms have been omitted for the sake of clarity. (B) Theoretical model based on the X-ray geometry used to evaluate the noncovalent interactions. Distances in Å

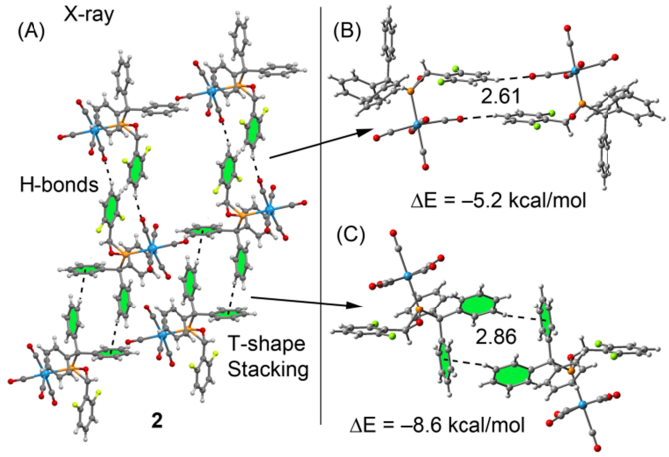

Fig. 8 (A) Partial view of the crystal packing in **2**. (B and C) Theoretical models of the self-assembled dimers based on the X-ray geometry used to evaluate the noncovalent interactions. Distances in Å.

A representative fragment of the crystal packing of compound **2** is shown in Fig. 8, where the disordered solvent molecule has been omitted. Two important self-assembled dimers are observed in the solid state. One of both is dominated by two equivalent W–CO···H–C hydrogen bonds (see Fig. 8B) and the other is characterized by the presence of two symmetrically equivalent T-shaped stacking interactions (or C–H/π interactions, see Fig. 8C). We have evaluated the binding energies of both self-assembled dimers, which are ΔE = –5.2 kcal/mol and ΔE = –8.6 kcal/mol for the H-bonded and T-shaped stacked dimers, respectively. The latter is more favourable than the former likely due the orientation of the interacting molecules allowing a higher contribution of long range dispersion interactions.

For compound **3**, the exploration of the crystal packing reveals the existence of two important dimers. One dimer is formed by means of two equivalent W–CO···H–C hydrogen bonds (see Fig. 9A). This self-assembled dimer interacts with another one by means of an antiparallel stacking interaction involving the trifluorophenyl rings. We have evaluated energetically both interactions (see Fig. 9B and C). The binding energy of the stacking interaction is ΔE = –8.1 kcal/mol, which is stronger than expected due to the contribution of an ancillary C–F···H–C hydrogen bond (2.77 Å, see Fig. 9B). The interaction energy of the self-assembled dimer that is dominated by the H-bonds is ΔE = –6.4 kcal/mol. This interaction energy is larger in absolute value than the one computed for the same interaction (W–CO···H–C hydrogen bond) in compound **2** (ΔE = –5.2 kcal/mol see Fig. 8B), likely due to the different directionality. In compound **3** the C≡O···H angle that characterizes the H-bond is 85º. Therefore, the positive H atom is interacting with the negative belt of the oxygen atom, giving rise to a stronger interaction compared to compound **2** where the angle is 178º.

Finally, a representative fragment of the crystal packing of compound **4** is shown in Fig. 10. The solid state structure is basically dominated by two interactions: (i) an antiparallel C–F···C–F and intermolecular W–CO···π interactions (see Fig.

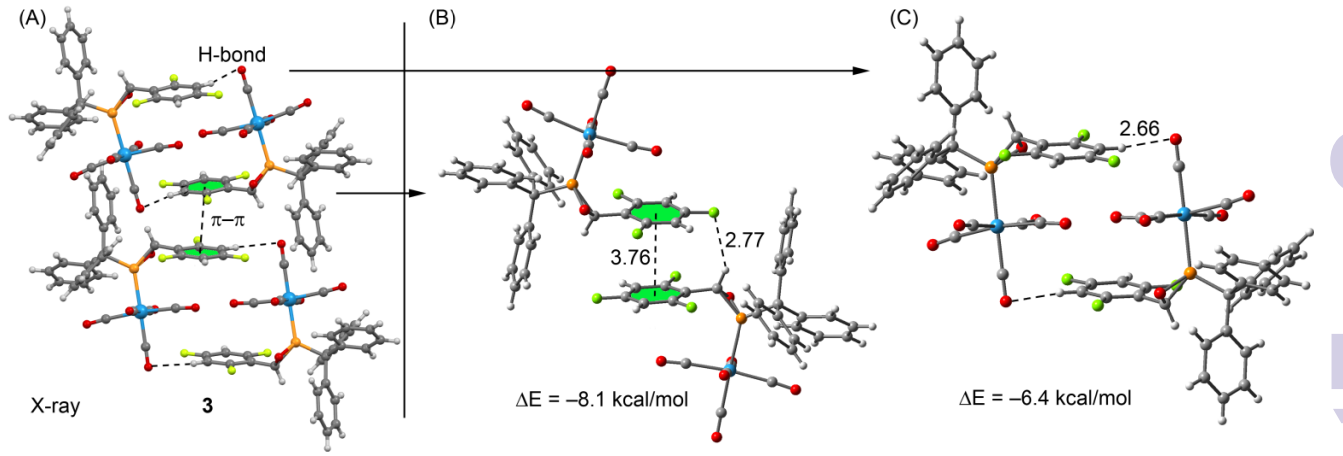

Fig. 9 (A) Partial view of the crystal packing in **3**. (B and C) Theoretical models of the self-assembled dimers based on the X-ray geometry used to evaluate the noncovalent interactions. Distances in Å

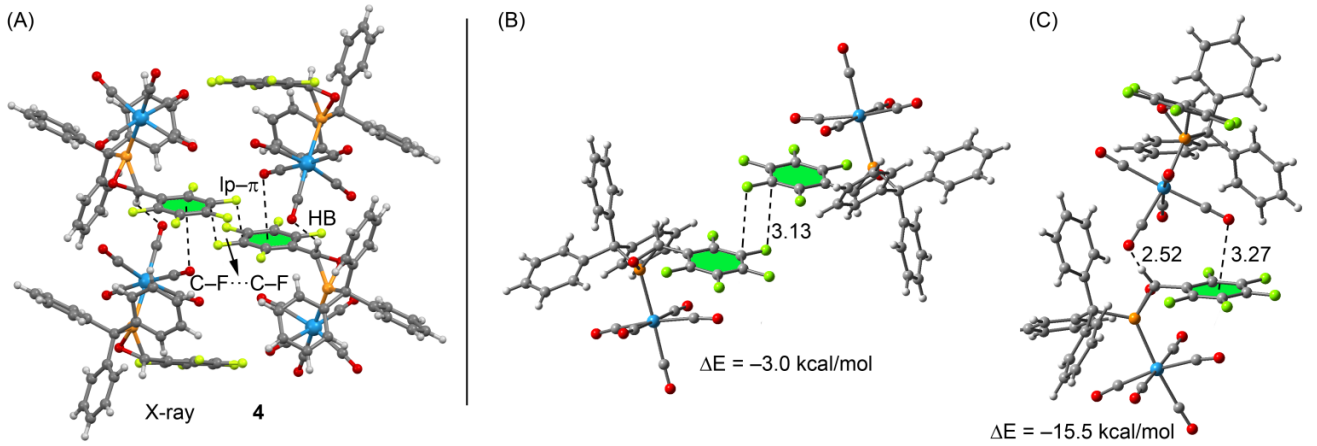

Fig. 10 (A) Partial view of the crystal packing in **4**. (B and C) Theoretical models of the self-assembled dimers based on the X-ray geometry used to evaluate th noncovalent interactions. Distances in Å.

10A) involving the pentafluorophenyl ring. Therefore the electron deficient pentafluorophenyl moiety establishes an intramolecular lp–π interaction by one side of the ring and an intermolecular lp–π interaction by the opposite side of the ring. We have evaluated theoretically both interactions and the energetic results are also included in Fig. 10. It can be observed that the antiparallel C–F···C–F interaction is ΔE = –3.0 kcal/mol, confirming the importance of this interaction in the solid state. Moreover the other intermolecular dimer under consideration that combines W–CO···π and H-bond interactions (see Fig. 10C) exhibits a large and negative interaction energy (ΔE = –15.5 kcal/mol) as a consequence of the contribution of long range dispersion interactions in addition to the W–CO···π and H-bond contacts. Interestingly, all compounds **1**–**4** exhibit W–CO···H–C hydrogen bonds in the solid state that influence the crystal packing. Moreover, compounds **1** and **4** also present intermolecular W–CO···π interactions in good agreement with the interaction energies summarized in Table 1 and the short intramolecular distances observed for both the π-acidic and π-basic rings. In compound **2** and **3**, intermolecular W–CO···π interactions are not observed. Instead π–π and T-shape stacking interactions are present influencing the final architecture of both compounds in the solid state.

4. Conclusions

In our previous communication we reported the synthesis and X-ray characterization of four new tungsten-oxaphosphirane complexes with close CO···π(arene) contacts. Unexpectedly, the phenyl substituted oxaphosphirane complex showed the shortest CO···π distance in the solid state, which was similar to the one observed for the pentafluorophenyl derivative. We rationalized the affinity of the M–CO moiety for both electron rich and electron deficient rings considering the duality of the CO···π interaction (i.e., δ^-–π interaction with the π-acidic and δ^+–π interaction with the π-basic arene) by means of several computational tools. In this manuscript we have further analysed the interaction using additional calculations (energetic and geometric features of intermolecular complexes **5**–**19**) and examining the CSD. To this respect, we have found a significant number of structures exhibiting W–CO···π interactions with low β angles that were not considered in the previously reported search. Moreover, we have analysed and rationalized the counterintuitive behaviour of the ^{31}P–NMR chemical shifts taking into consideration charge transfer effects between the π system and the CO ligand. Finally, we have analysed the solid state architecture of compounds **1**–**4** and evaluated theoretically the main forces that govern the crystal packing. Interestingly, compounds **1** and **4** also exhibit intermolecular W–CO···π interactions in the solid state.

Notes and references

[a] Institut für Anorganische Chemie, Rheinische Friedrich-Wilhelms-Universität Bonn, Gerhard-Domagk-Str. 1, 53121 Bonn, Germany. E-mail: r.streubel@uni-bonn.de

[b] Departament de Química, Universitat de les Illes Balears, Crta de Valldemossa km 7.5, 07122 Palma de Mallorca (Baleares), Spain. E-mail: toni.frontera@uib.es.

† Electronic supplementary information (ESI) available: Cartesian coordinates of the optimized complexes **5**–**19** See DOI: 10.1039/c000000x/

‡ We thank to MINECO of Spain (projects CTQ2014-57393-C2-1-P and CSD2010-00065, FEDER funds) for financial support. We also thank the DFG foundation (STR 411/29-1 and SFB 813 "Chemistry at Spin Centers") and cost action CM1302 "Smart Inorganic Polymers" (SIPs) for financial support.

1 H. J. Schneider, *Angew. Chem. Int. Ed.* 2009, **48**, 3924 – 3977

2 J. W. Steed and J. L. Atwood, *Supramolecular chemistry*, Wiley, Chichester, 2000.

3 (a) E. A. Meyer, R. K. Castellano and F. Diederich, *Angew. Chem. Int. Ed.* 2003, **42**, 1210 – 1250; (b) H. J. Schneider and A. Yatsimirsky, *Chem. Soc. Rev*. 2008, **37**, 263 – 277

4 (a) L. M. Salonen, M. Ellermann and F. Diederich, *Angew. Chem. Int. Ed*., **2011**, *50*, 4808 – 4842.
5 (a) M. Egli and S. Sarkhel, *Acc Chem Res*., 2007, **40**, 197–205. (b) T. J. Mooibroek, P. Gamez and J. Reedijk, *CrystEngComm*., 2008, **10**, 1501–1515.
6 J. Zukerman-Schpector and E. R. T. Tiekink, *CrystEngComm* 2014, **16**, 6398-6407
7 S. Sarkhel, A. Rich and M. Egli, *J. Am. Chem. Soc*., 2003, **125**, 8998–8999; (b) J. P. Gallivan and D. A. Dougherty, *Org Lett*. 1999, **1**, 103–105.
8 M. Egli and R. V. Gessner, *Proc. Natl. Acad. Sci*., 1995, **92**, 180–184.
9 Y. Li, L. B. Snyder and D. R. Langley, *Bioorg. Med. Chem. Lett*. 2003, **13**, 3261–3266.
10 I. Alkorta, I. Rozas and J. Elguero, *J. Org. Chem.,* 1997, **62**, 4687-4691.
11 B. W. Gung, Y. Zou and Z. Xu, *J. Org. Chem*. 2008, **73**, 689–693.
12 I. Caracelli, J. Zukerman-Schpector and E. R. T. Tiekink, *Coord. Chem. Rev*. 2012, **256**, 412-438.
13 F. H. Allen, *Acta Cryst*., 2002, **B58**, 380-388.
14 (a) A. Özbolat, G. von Frantzius, M. Nieger and R. Streubel, *Angew. Chem. Int. Ed.,* 2007, **46**, 9327; (b) V. Nesterov, G. Schnakenburg, A. Espinosa and R. Streubel, *Inorg. Chem*., 2012, **53**, 12343–12349. (c) J. Marinas-Pérez, H. Helten, G. Schnakenburg and R. Streubel, *Chem. Asian J*., 2011, **6**, 1539–1545.
15 C. Murcia-García, A. Bauzá, G. Schnakenburg, A. Frontera and R. Streubel,' *CrystEngCommun,* 2015, **17**, 1769–1772
16 R.Ahlrichs, M. Bär, M. Haser, H. Horn and C. Kölmel, *Chem. Phys. Lett*., 1989, **162**, 165–169.
17 S. Grimme, J. Antony, S. Ehrlich and H. Krieg, *J. Chem. Phys*., 2010, **132**, 154104– 154119.
18 S. F. Boys and F. Bernardi, *Mol. Phys.* 1970, **19**, 553–566.
19 R. F. W. Bader, *Chem. Rev.* 1991, **91**, 893–928.
20 AIMAll (Version 13.11.04), T. A. Keith, TK Gristmill Software, Overland Park KS, USA **2013**.
21 S. Maurer, C. Burkhart and G. Maas, *Eur. J. Org. Chem*., 2010, **2010**, 2504–2511.
22 M. R. Awang, J. C. Jeffery and F. G. A. Stone, *J. Chem. Soc., Dalton Trans*. 1983, 2091–2098.
23 J. A. B. Abdalla, I. M. Riddlestone, J. Turner, P. A. Kaufman, R. Tirfoin, N. Phillips, S. Aldridge, *Chem.-Eur. J*. 2014, **20**, 17624-17634.
24 R. Streubel, A. W. Kyri, L. Duan and G. Schnakenburg, *Dalton Trans*. 2014, **43**, 2088–2097.